Brain Lesion Detection: An Architecture Based On Convolution Neural Network

Ullas Kumar Agrawal[1], Pankaj Kumar Mishra[2*] Mohan Awasthy[3*]

[1]PhD Scholar, Electronics & Telecommunication, Rungta College of Engineering and Technology, Bhilai, INDIA Email:ullasagrawal361@gmail.com

[2]Professor, Rungta College of Engineering & Technology, Bhilai,(C.G.) INDIA Email:pmishra1974@yahoo.co.in

[3]Principal and Professor Rungta College of Engineering and Technology Bhilai C.G India e-mail, , Email awasthymohan@gmail.com

Abstract

MRI based lesion detection is an essential step for computer aided diagnosis to detect brain lesion. There are several types of tissues, skull portion in brain MRI images, which lead to false detection of brain lesion. To get appropriate lesion detection segmentation architecture based on Convolution Neural Network (CNN) is proposed in the study. Here, 2450 3D RGB images are taken from The Cancer Genome Atlas (TCGA), where 2400 images are used from 104 patients for training purpose and 50 images are taken from six patients for testing purpose. From the test images the architecture achieved accuracy (99.1%), dice similarity (85.4%), jaccard index (74.8%), Mathews correlation coefficient (82.2%), sensitivity (89.7%), specificity (99.3%), and precision (82.3%) with 95% confidence interval. Besides, the receiver operating characteristic (ROC) curve also plotted with highest 97.22% area, which proves the constancy and reliability of the architecture. The proposed CNN based architecture detects the accurate lesion from brain MRI 3D RGB images.

Keywords: The Cancer Genome Atlas, Convolution Neural Network, Brain lesion, Segmentation, Border removing, Artefacts removing.

Highlights

- Precise brain lesion segmentation by CNN based deep learning architecture.
- TCGA dataset is used for training and testing.
- Assessment of seven performance parameters.
- ROC curve analysis for each of six test patients.

1. Introduction

Brain lesions are abnormal tissues that are formed inside the skull by the adjacent brain tissues and directly influence normal life. These abnormal tissues tend to develop irregularly in the brain and create stress in the skull [1]. Due to the stress, the lesion causes various disorders in the brain that disturbs human activities. Indications of such disorders are found by dizziness, headache, fainting attacks, paralysis and so on. [2]. though, the existence of lesions in vital area can be cured by altered treatment approaches such as medicine, radiation therapy, chemotherapies. Instead of surgery [3,4]. In 2019, it was predicted that within approximately 700 thousand public with brain lesions, approximately 86 thousand of these cases were identified in America [5].Out of them, 60,490 were benign and 25,510 were malignant, within them only 35.8% malignant patients survived [6].

Brain lesions are originated from brain tissues or from different organs, which are classified by primary and secondary lesions. In the brain glial tissues, gliomas are formed, which are mainly primary brain lesions. Gliomas are classified by low-grade-gliomas (LGG) and high-grade-gliomas (HGG) lesions. There are two WHO subtypes of LGG, those are grade II and III brain lesions. Grade I can be cured by surgery but, grade II and III are aggressive malignant lesion and are developed to higher-grade lesion[4,7]. The high grade gliomas are an destructive type of malignant brain lesion which have poor survival prognosis. Magnetic Resonance Imaging (MRI) is a chief diagnostic technique for brain lesion analysis, observation[8].So, early detection by MRI of brain lesion can save more lives.

LGG treatment is divisive and remains not consistent, and the current brain lesion detection is imprecise at observing patient consequences and creates inter-observer variability [9]. Automated 2D and 3D brain lesions segmentation can achieve the result faster and deliver a precise detection for further lesion investigation and observation. Recently, deep learning techniques were studied in the area of medical applications. The network models of deep learning involves of several hidden layers. Besides, this technique automatically learns from the selected database[5]. Inside various deep learning

ISSN: 0975-3583, 0976-2833 VOL 12, ISSUE 03, 2021

model Convolution neural network (CNN) based computer aided diagnosis (CAD)can achieve better accuracy for segmentation result in 2D [10] and 3D biomedical images [11].

Earlier studies have employed different CAD network architecture based on machine learning and deep learning to segment the brain lesion to solve the difficulty based on radiologists. In 2015, Nabizadeh et al. [12] proposed a MRI slice recognition method by histogram asymmetry, which can classify the slice that the slice includes lesion or not. Then by using texture based feature, segmentation was achieved and classification was achieved by support vector machine (SVM), k-nearest neighbour principle (KNN), sparse representation classifier (SRC) [13], nearest subspace classifier (NSC), and k-means clustering methods. In the study classification performance were evaluated by sensitivity, specificity and accuracy parameters.

In 2016, Pereira et al. [14] recommended a CNN based automated segmentation method to BRATS 2013 and BRATS 2015 database. In the study, dice similarity (DSC), PPV and sensitivity were measured, as segmentation performance of complete, core and enhancing regions of brain lesions. In the same year, Hasan et al. [15] applied 3D active contour without edge to segment the lesion. In the study, feature extraction and classification were done. In the study 89% ± 4.7% highest segmentation accuracy was achieved. Besides, in that year Isselmou et al. [16] used threshold segmentation and morphological operations to detect brain lesions in MRI images. In the study performance evaluation was achieved and graphical user interface (GUI) was also created.

In 2017, Dong et al. [17] proposed CNN based U-Net to segment brain lesion on 3D MRI images of BRATS 2015 datasets. In the study, cross validation was applied and the results of the proposed technique were compared with other techniques. Besides, DSC was evaluated for complete, core and enhancing brain lesions. In that year, Hussain et al [18] used deep CNN to segment brain lesions in BRATS 2013 datasets. Besides, DSC, sensitivity and specificity were evaluated.

In 2018, Myronenko [19] applied CNN based encoder-decoder architecture to segment brain lesions on BRATS 2018 dataset, where larger encoder was used for feature extraction and smaller decoder was used for segmentation. In the study, variation-auto encoder was also added to the network for regularization purpose. Besides, DSC and Hausdorff measurement were evaluated for performance measurement. In the same year, Naceur et al. [20] proposed CNN based incremental XCNet algorithm and applied ELOBA-λ algorithm to segment brain lesion on BRATS 2017 dataset. In the study, various performance parameters were evaluated can benchmarked with others results. In that year, Iqbal et al. [21] applied three networks architecture based on CNN on BRATS 2015 datasets. Besides, the performance were evaluated and benchmark was evaluated.

In 2019, Marcinkiewicz et al. [22] applied fully CNN based U-Net on BRATS 2018 datasets. In the study, T2-FLAIR, T2 and T1Gd slices are used to segment peritumoral-edema, lesion core and enhancing lesion respectively. In the study, performance are evaluated for enhancing lesion, whole lesion and lesion core.The presentation of the paper is as follows. Deep learning architecture based on CNN is explained in section 2. Performance parameters are elaborated in section 3. The achieved results are shown in section 4. The results are discussed in section 5. At last the conclusion is presented.

2.Materials and methods

The Cancer Genome Atlas (TCGA) dataset contains brain MRI 3D RGB image data of 110 patients. There are approximately 1250 images, which contains brain lesion and approximately 1250 normal images of those patients, which do not contain lesion. In the study, 1200 abnormal 3D RGB images and 1200 normal images from 104 patients are used for training purpose. For testing purpose, 50 different images from six different patients are used [7]. The flow-chart is represented in Fig. 1.

ISSN: 0975-3583, 0976-2833 VOL 12, ISSUE 03, 2021

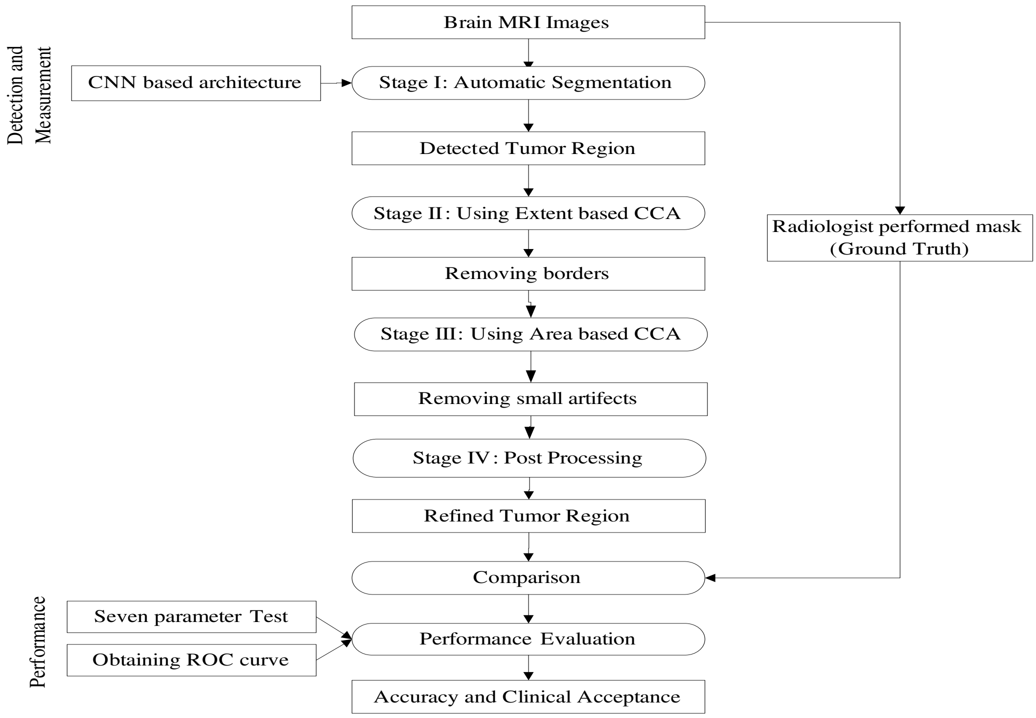

Fig. 1. Flow chart showing three stages: automatic segmentation, border removing, and post-processing. The performance block is used to evaluate the results.

1.1 Segmentation

In the study, Convolution Neural Network (CNN) and transposed convolution are used as the base function. Here a CNN based architecture is used to segment the brain lesion from the 3D RGB complete image. The explanation of the architecture is followed.

1.1.1 CNN based architecture

Deep learning (DL) is a part of Machine learning, where the computer can learn from the supervised dataset. In DL, the machine evaluates each image for image processing. From the evaluation, the machine gather some experience, which is nothing but some digits. At the time of testing, the same calculation is done again and is matched the experience gained from training by the machine. Now, in case of CNN based architecture the function for the calculation is CNN layer. The CNN based architecture is followed in Fig. 2 [23-25]. The training process are shown in Fig. 3. From the figure, the accurate learning process of the proposed architecture are observed by the training accuracy and the training loss are observed.

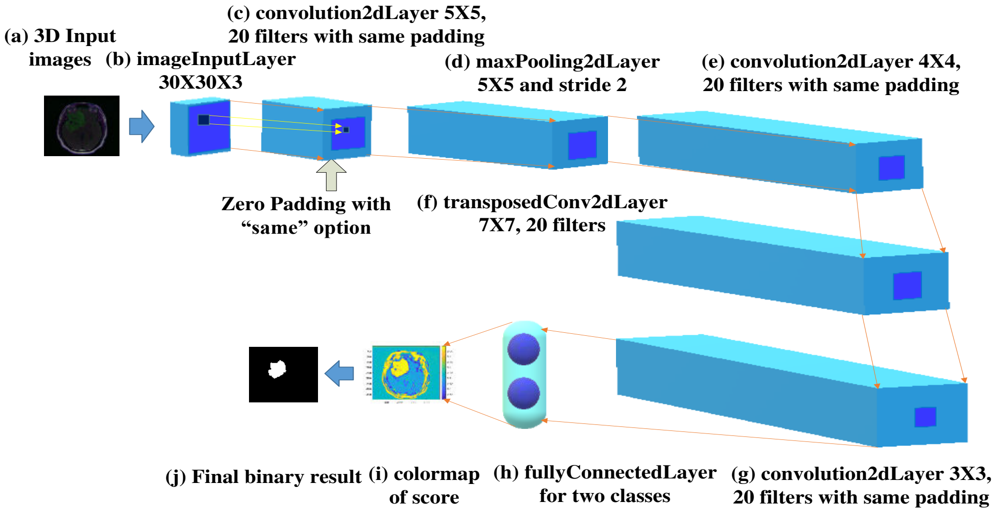

Fig. 2. The architecture of the CNN based hybrid approach.

ISSN: 0975-3583, 0976-2833 VOL 12, ISSUE 03, 2021

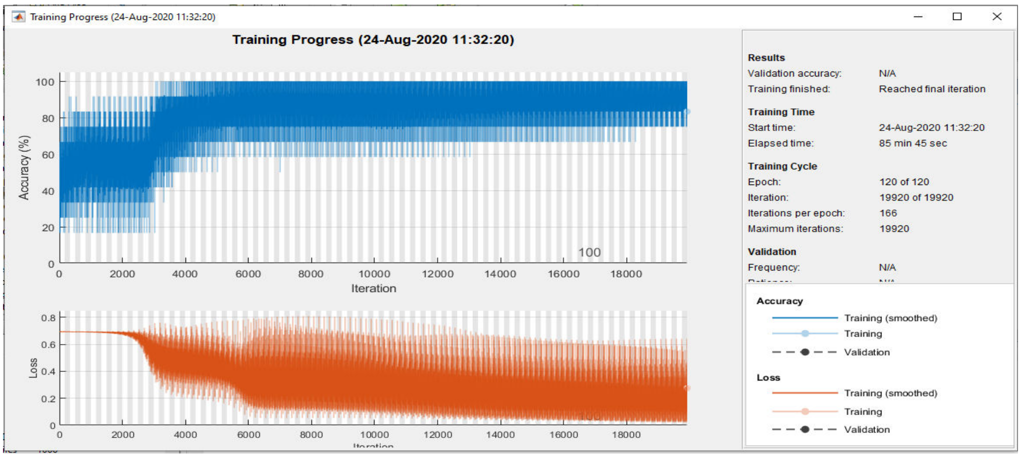

Fig. 3. The training process of the CNN based architecture.

1.2 Border removing

After achieving the binary result from the CNN based architecture, the binary image contains some borders, which are not the lesion. The borders are the part of the brain skull. Fig. 4(a) describes the binary image achieved from CNN based architecture and Fig. 4(b) shows the binary images after removing the borders by connected component analysis (CCA). In the process the CCA is worked based on extent of each connected component. Extent is the ratio of area and area of bounding box. There are different threshold value for each images. In the study, the value of extent is chosen 0.56 after observing all images.

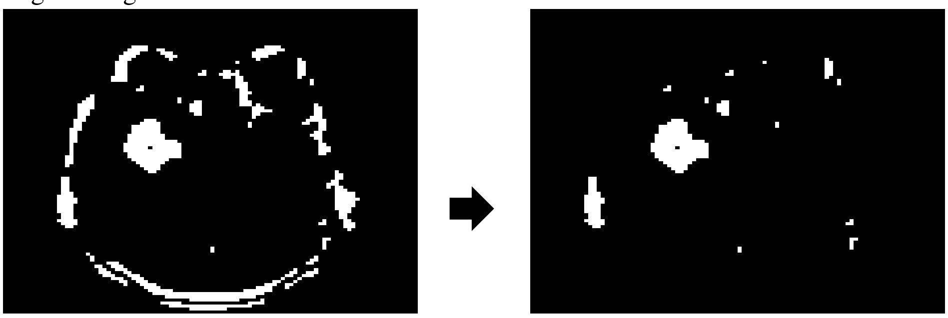

(a) Segmented image by using CNN

(b) After removing Border

Fig. 4. The Border removing process

1.3 Artefacts removing

After removing the border from the binary images there are several small artefacts. Fig. 5(a) shows the image after border removing and Fig. 5(b) elaborates the binary image after removing small artefacts. The process is done on area based CCA. There are diverse value for each image. A threshold value is arbitrarily chosen. The value is 45% of the value of the highest value.

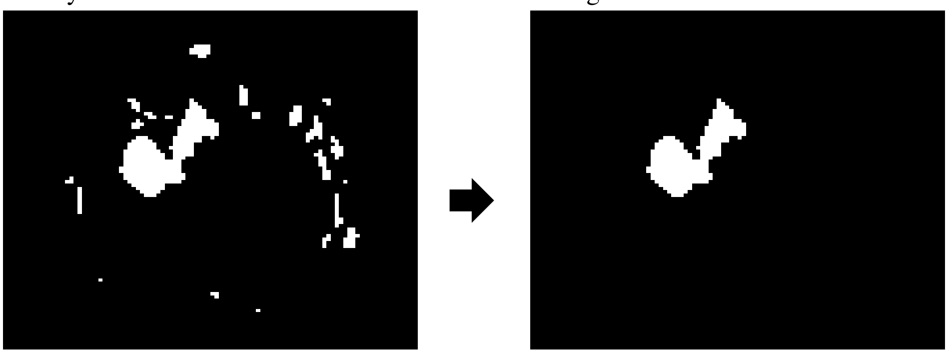

(a) Image after border removing

(b) After artefacts removing

Fig. 5. The artefacts removing process

ISSN: 0975-3583, 0976-2833 VOL 12, ISSUE 03, 2021

1.4 Post-processing

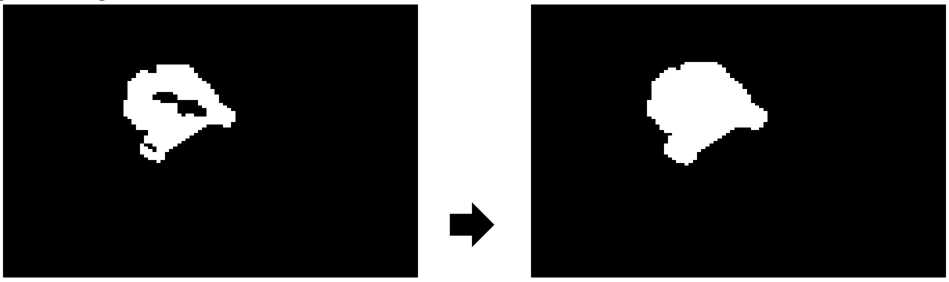

(a) After removing artefacts **(b) Image after post-processing**

Fig. 6. The Post-processing process

After removing small artefacts, post-processing is done to smooth the image. Fig. 6(a) describes the binary image after removing small artefacts and Fig. 6(b) shows the final image after post-processing. In the stage, erosion, dilation is used with the morphological disk operation with the radius one, and image gap filling is also done. For image analysis MATLAB® 2018a (Math Works, Inc., Natick, MA) software was used. The PC configuration of our system is as follows: Intel (R) Pentium (R) N-3710 CPU Processor, 1.60 GHz, and 4 GB RAM, with Windows-10 Operating System.

2. **Performance evaluation** The performance evaluation is based on two different parts. Those are followed,

i. Statistical summary analysis.
ii. Seven parameters are evaluated between the CNN based segmentation results and the GT binary images. Those are Accuracy, Dice similarity coefficient (DSC), Jaccard index (JI), Mathews correlation coefficient (MCC), Sensitivity, Specificity, and precision. The parameters are described in the Table 2.
iii. Receiver Operating Characteristic (ROC) curve analysis.

Based on true positive (T_P), true negative (T_N), false positive (F_P), false negative (F_N) the performance parameters of the CNN based architecture is presented. The seven parameters are described in Table 2.

Table 2

Elaboration of seven performance constraints.

Sl. No.	Performance Parameters	Formula	Description
1	Accuracy	$\text{Accuracy} = (T_P + T_N)/(F_N + F_P + T_P + T_N)$	evaluates the intimacy of a result
2	Dice similarity coefficient	$\text{DSC} = (2 * T_P)/(2 * T_P + F_P + F_N)$	measures the probabilistic similarity
3	Jaccard index	$\text{JI} = \text{DSC}/(2 - \text{DSC})$	
4	Appropriate Matthews correlation coefficient	$\text{MCC} = \frac{(T_P * T_N - F_P * F_N)}{\sqrt{((T_P + F_P) * (T_P + F_N) * (T_N + F_P) * (T_N + F_N))}}$	shows the correlation index
5	Sensitivity	$\text{Sensitivity} = T_P/(T_N + F_N)$	measures the proportion of the positive result
6	Specificity	$\text{Specificity} = T_N/(T_N + F_P)$	measures the proportion of a negative result
7	Precision	$\text{Precision} = T_P/(T_P + F_P)$	describes the relevancy of the achieved result

DSC – Dice similarity coefficient, JI – Jaccard index.

ISSN: 0975-3583, 0976-2833 VOL 12, ISSUE 03, 2021

3. Result

Table 3 describes the statistical summary of the proposed architecture, with respect to GT. In the Table 4, the performance parameters results are described. From Fig.7, it is observed that, the 3D RGB test images of four patient out of six test patient images, In the figure, the binary GT mask images of corresponding images are shown. In the third row the architecture based results are shown. Then, in the fourth row the overlay images based on GT mask are provided, then the overlay images based on segmentation results are shown. Finally, both overlay are compared, where yellow describes the GT overlay and the red marking describes the proposed architecture results. Fig. 8 shows the ROC curve with the value for each of six patients.

Table 3

Statistic summary of the brain lesion's area (pixel^2) CNN based technique and the GT.

Method	Interpretations			
	Mean	**Variance**	**SD**	**Median**
GT	388.440	64955.762	254.864	282.500
CNN based technique	**361.520**	**65265.030**	**255.470**	**259.500**

CNN – Convolution Neural Network, GT – Ground Truth, DSC – Dice similarity coefficient, JI – Jaccard index.

Table 4

Evaluation of performance parameters between CNN based technique and the GT with 95% CI.

Method	Interpretations					
	Accuracy	**DSC**	**JI**	**Sensitivity**	**Specificity**	**Precision**
CNN	0.991±0.002	0.854±0.012	0.748±0.018	0.897±0.021	0.993±0.002	0.823±0.019

CNN – Convolution Neural Network, GT – Ground Truth, DSC – Dice similarity coefficient, JI – Jaccard index, CI – confidence interval.

ISSN: 0975-3583, 0976-2833 VOL 12, ISSUE 03, 2021

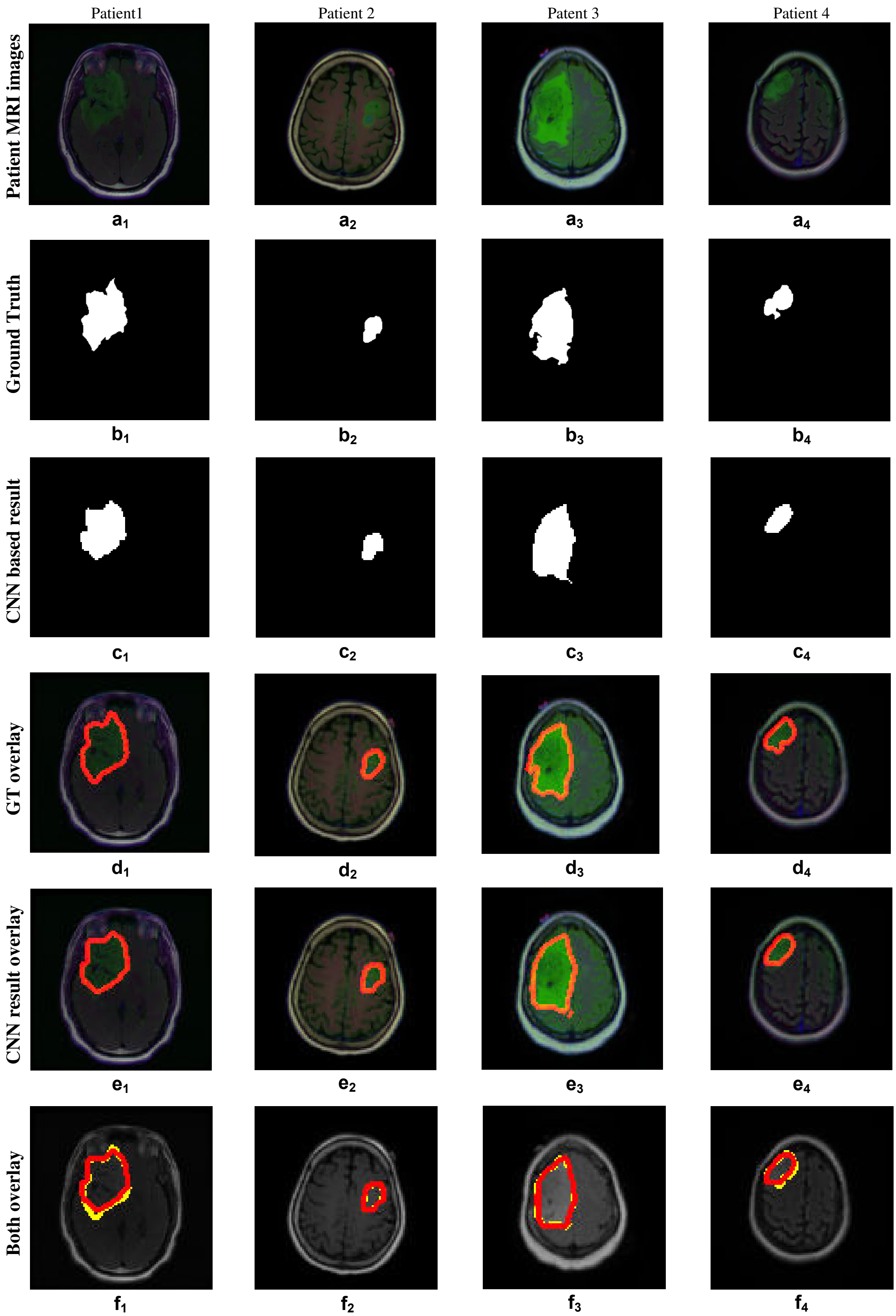

Fig. 7. A comparison between overlay images from four different patients (Patient 1 to Patient 4) produced by CNN based segmentation techniques and the GT. a_1-a_4 shows the test images; b_1-$b_4$are GT binary mask images; c_1-c_4 are binary result images.d_1-d_4 are overlay of GT images; e_1-e_4 are overlay of result images; f_1-f_4 are comparison of both of GT overlay (Yellow) detected lesions using CNN based overlay (Red) , respectively.

ISSN: 0975-3583, 0976-2833 VOL 12, ISSUE 03, 2021

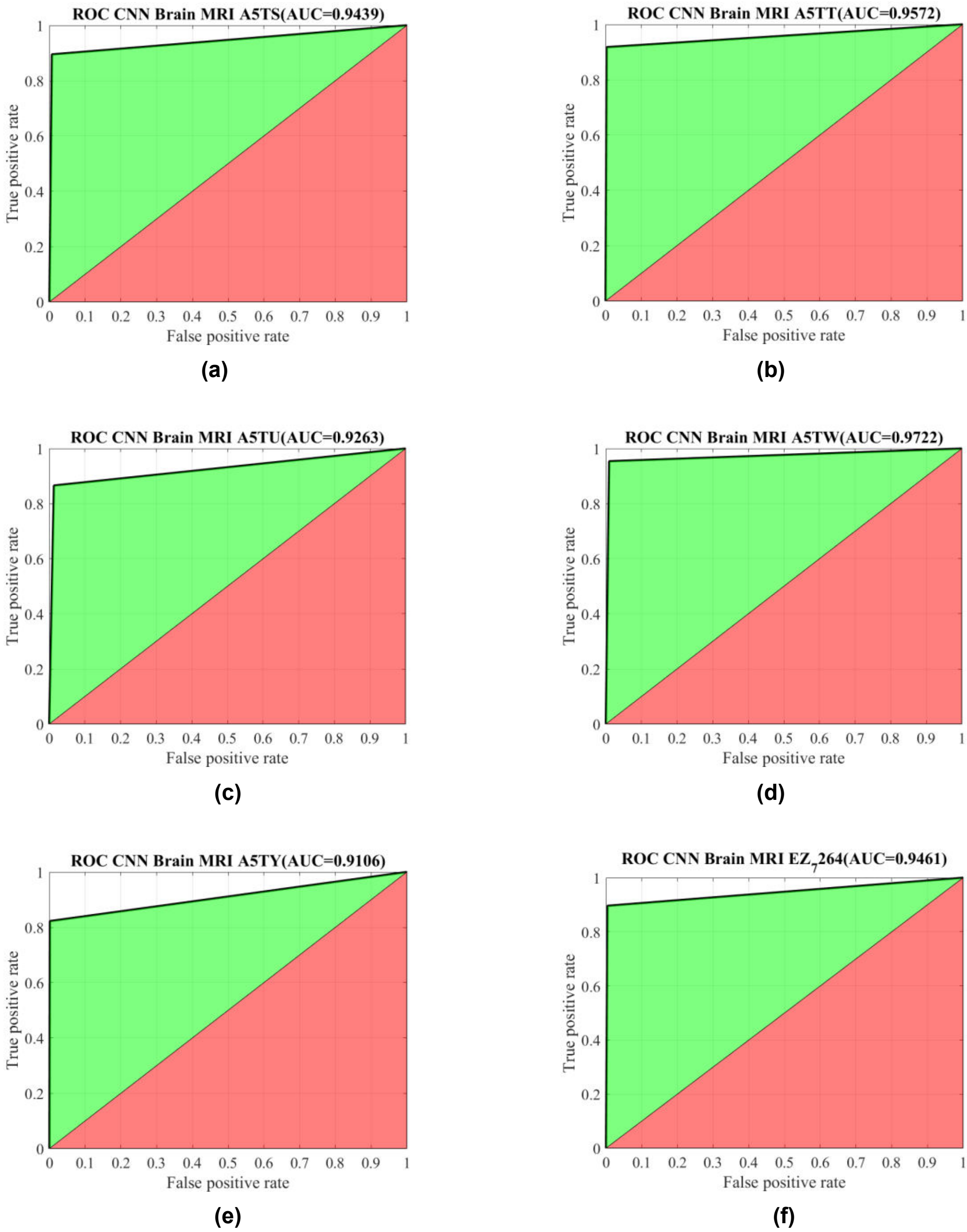

Fig. 8. ROC plots of patients, namely; (a) Patient 1, (b) Patient2, (c) Patient 3, (d) Patient 4, (e) Patient 5, and (f) Patient 6 with respect to the GT.

4. Discussion

In the study, CNN based deep learning architecture is proposed to detect brain lesion and the achieved result is compared with the GT. The complete process are discussed in the section.

4.1 A note on segmentation technique

In the study, CNN based architecture is selected. From, previous studies [17-22], the efficiency of CNN based deep learning is found. In the architecture, CNN not only learn the features of images, but also, reduce the loss at the training. In the architecture the padding option makes the architecture more flexible than, others CNN based approaches. Here, 3D RGB images are trained and different 3D RGB images are tested.

ISSN: 0975-3583, 0976-2833 VOL 12, ISSUE 03, 2021

4.2 A note on border removing

From the achieved results are binary images. The binary images consisted skull border. The ratio of area and bounding box area of those borders are not very high as it is part of skull margins. The border are neither the lesion nor the tissues. To achieve the actual lesion, those borders are erased by applying CCA based on extent.

4.3 A note on artefacts removing

After removing borders, still there are small artefacts in the binary images. Those are not the abnormal tissues. The artefacts are noise in the results. Those are removed by applying CCA based on area. The threshold is selected based on the percentage of the highest area component.

4.4 A note on post-processing

Finally, the morphological disk shape operation is applied to smooth the images and to black spots inside the binary images are removed from the brain lesion area.

4.5 A note on performance

Table 3 and Table 4 illustrate the performance of the architecture based on GT binary images. Table 3, shows that the achieved area of the brain lesion is closer to the GT area. From Table 4, the performance of the proposed architecture is observed. Here, accuracy, DSC, JI, MCC, sensitivity, specificity and precision are evaluated. Those performances are achieved in previous studies [13-15, 17-21] with different train and test images.

Further, the CNN based proposed architecture requires less time and is robust to noise due to its complicacy. Thus, the architecture is able to accurate detection of brain lesion.

4.6 A note on ROC analysis

Based on the binary segmentation results, six different ROC curves are plotted with respect to GT. The true positive rate and the false positive rate are the two axes of the graph. Fig. 8 describes the area under curve (AUC) of the ROC [26]. For six patients, the highest AUC is 0.9722 and lowest is 0.9106. The graphs proves the correlation between the proposed architecture results and the GT.

4.7 Strength, weakness, and extensions

In the study, CNN based robust architecture is proposed. Performance is evaluated with 95% CI for all test images and ROC curve with AUC is achieved for each patient. The architecture can be modified. Here, feature extraction and classification are not achieved.

5. Conclusion

The study proposed a robust architecture to segment brain lesion in MRI images by using deep learning-based CAD model. The proposed model was evaluated on 50 MRI images obtained from 6 patients. The results indicate that 99.1% segmentation accuracy was achieved by the proposed approach. The ROC graph further describes the consistency of the results. The AUC value was found to be 97.22%. It is concluded that CNN-based CAD model can be used in routine clinical scenario for detecting lesions in brain MRI images. In future multi-modal imaging with better ground truth validations may be developed to improve the performance of CAD systems.

References

1. Grisold, W., &Grisold, A. Cancer around the brain. NeurooncolPract. 2014; 1 (1): 13-21.
2. Kheirollahi, M., Dashti, S., Khalaj, Z., Nazemroaia, F., &Mahzouni, P. (2015). Brain tumors: Special characters for research and banking. Advanced biomedical research, 4.
3. Lukoff, J., & Olmos, J. (2017). Minimizing medical radiation exposure by incorporating a new radiation “Vital Sign” into the electronic medical record: quality of care and patient safety. The Permanente Journal, 21.
4. Smoll, N. R., Schaller, K., &Gautschi, O. P. (2013). Long-term survival of patients with glioblastoma multiforme (GBM). Journal of Clinical Neuroscience, 20(5), 670-675.
5. Toğaçar, M., Ergen, B., &Cömert, Z. (2020). BrainMRNet: Brain tumor detection using magnetic resonance images with a novel convolutional neural network model. Medical Hypotheses, 134, 109531.
6. Ostrom, Q. T., Cioffi, G., Gittleman, H., Patil, N., Waite, K., Kruchko, C., &Barnholtz-Sloan, J. S. (2019). CBTRUS statistical report: primary brain and other central nervous system tumors diagnosed in the United States in 2012–2016. Neuro-oncology, 21(Supplement_5), v1-v100.
7. Buda, M., Saha, A., &Mazurowski, M. A. (2019). Association of genomic subtypes of lower-grade gliomas with shape features automatically extracted by a deep learning algorithm. Computers in biology and medicine, 109, 218-225.
8. Myronenko, A. (2018, September). 3D MRI brain tumor segmentation using autoencoder regularization. In International MICCAI Brainlesion Workshop (pp. 311-320). Springer, Cham.

ISSN: 0975-3583, 0976-2833 VOL 12, ISSUE 03, 2021

9. Cancer Genome Atlas Research Network. (2015). Comprehensive, integrative genomic analysis of diffuse lower-grade gliomas. New England Journal of Medicine, 372(26), 2481-2498.
10. Chen, L. C., Zhu, Y., Papandreou, G., Schroff, F., & Adam, H. (2018). Encoder-decoder with atrous separable convolution for semantic image segmentation. In Proceedings of the European conference on computer vision (ECCV) (pp. 801-818).
11. Milletari, F., Navab, N., Ahmadi, S. A. V., & V-Net. Fully convolutional neural networks for volumetric medical image segmentation. In Proceedings of the 2016 Fourth International Conference on 3D Vision (3DV) (pp. 565-571).
12. Nabizadeh, N., &Kubat, M. (2015). Brain tumors detection and segmentation in MR images: Gabor wavelet vs. statistical features. Computers & Electrical Engineering, 45, 286-301.
13. Wright, J., Yang, A. Y., Ganesh, A., Sastry, S. S., & Ma, Y. (2008). Robust face recognition via sparse representation. IEEE transactions on pattern analysis and machine intelligence, 31(2), 210-227.
14. Pereira, S., Pinto, A., Alves, V., & Silva, C. A. (2016). Brain tumor segmentation using convolutional neural networks in MRI images. IEEE transactions on medical imaging, 35(5), 1240-1251.
15. Hasan, A. M., Meziane, F., Aspin, R., &Jalab, H. A. (2016). Segmentation of brain tumors in MRI images using three-dimensional active contour without edge. Symmetry, 8(11), 132.
16. Zhang, S., & Xu, G. (2016). A novel approach for brain tumor detection using MRI Images. Journal of Biomedical Science and Engineering, 9(10), 44-52.
17. Dong, H., Yang, G., Liu, F., Mo, Y., & Guo, Y. (2017, July). Automatic brain tumor detection and segmentation using U-Net based fully convolutional networks. In annual conference on medical image understanding and analysis (pp. 506-517). Springer, Cham.
18. Hussain, S., Anwar, S. M., & Majid, M. (2017, July). Brain tumor segmentation using cascaded deep convolutional neural network. In 2017 39th Annual International Conference of the IEEE Engineering in Medicine and Biology Society (EMBC) (pp. 1998-2001). IEEE.
19. Myronenko, A. (2018, September). 3D MRI brain tumor segmentation using autoencoder regularization. In International MICCAI Brainlesion Workshop (pp. 311-320). Springer, Cham.
20. Saouli, R., Akil, M., &Kachouri, R. (2018). Fully automatic brain tumor segmentation using end-to-end incremental deep neural networks in MRI images. Computer methods and programs in biomedicine, 166, 39-49.
21. Iqbal, S., Ghani, M. U., Saba, T., & Rehman, A. (2018). Brain tumor segmentation in multi-spectral MRI using convolutional neural networks (CNN). Microscopy research and technique, 81(4), 419-427.
22. Manish Pandey et.al. (2020) Review, Study & Modelling of Neuro-Fuzzy System, It's Performance Comparision Using Various Speech Databases for Recognition of Emotional States" Journal of Critical Reviews ISSN- 2394-5125 Vol 7, Issue 12,2020 pp 1231-1240 Impact Factor 1.091 Jalan ampang, Kuala Lumpur, malaysia
23. Marcinkiewicz, M., Nalepa, J., Lorenzo, P. R., Dudzik, W., &Mrukwa, G. (2018, September). Segmenting brain tumors from MRI using cascaded multi-modal U-Nets. In International MICCAI Brainlesion Workshop (pp. 13-24). Springer, Cham.
24. Goodfellow, I., Bengio, Y., Courville, A., &Bengio, Y. (2016). Deep learning (Vol. 1). Cambridge: MIT press.
25. Collobert, R. (2011, June). Deep learning for efficient discriminative parsing. In Proceedings of the fourteenth international conference on artificial intelligence and statistics (pp. 224-232).
26. Manish Pandey et.al. (2020)n Study & Scheme Of Neuro-Fuzzy System With Various Databases for Emotional States Recognition International Journal of Advanced Science and Technology I SSN: 2005-4238 Vol. 29, No. 7, (2020), pp. 804- Science and Engineering Research Support Society SERSC Australia 26